

Automatic Setae Segmentation from *Chaetoceros* Microscopic Images

HAIYONG ZHENG,* HONGMIAO ZHAO, XUE SUN, HUIHUI GAO, AND GUANGRONG JI

Department of Electronic Engineering, Ocean University of China, No. 238 Songling Road, Qingdao, Shandong 266100, China

KEY WORDS GSDAM; microscopic image segmentation; biomorphic characteristics; setae detection

ABSTRACT A novel image processing model Grayscale Surface Direction Angle Model (GSDAM) is presented and the algorithm based on GSDAM is developed to segment setae from *Chaetoceros* microscopic images. The proposed model combines the setae characteristics of the microscopic images with the spatial analysis of image grayscale surface to detect and segment the direction thin and long setae from the low contrast background as well as noise which may make the commonly used segmentation methods invalid. The experimental results show that our algorithm based on GSDAM outperforms the boundary-based and region-based segmentation methods Canny edge detector, iterative threshold selection, Otsu's thresholding, minimum error thresholding, K-means clustering, and marker-controlled watershed on the setae segmentation more accurately and completely. *Microsc. Res. Tech.* 77:684–690, 2014. © 2014 Wiley Periodicals, Inc.

INTRODUCTION

Chaetoceros species have a worldwide distribution, and they often dominate marine ecosystems (Lee and Lee, 2011; Tabassum and Saifullah, 2010). Some have caused important blooms in both oceanic and coastal habitats (Shevchenko and Orlova, 2010), which can make large and critical impacts on marine ecosystems, aquaculture as well as global climate, etc.

Identifying and classifying phytoplankton species accurately and rapidly play an important role in predicting and monitoring the algal blooms. The traditional method of phytoplankton taxonomy mainly relies on well-experienced experts using microscope based on the characteristics of biological morphology, which is time-consuming and laborious and cannot be applied to the large number of samples as well as on-site and in situ real-time analysis. Therefore, in the last two decades researchers have made many contributions on automatic identification and classification of phytoplankton using microscopic images.

However, prior to automatic identification, reliable segmentation of biomorphic characteristics should be performed (Jalba et al., 2004). *Chaetoceros* is mainly characterized by its chain-forming cells and their setae structures, and one of their most conspicuous characteristics is number of setae possessed per cell (Lee and Lee, 2011). Our goal in this article is to segment the setae from *Chaetoceros* microscopic images, which can be used for the further *Chaetoceros* automatic identification and classification.

Image segmentation has played an important role in computer vision, and its accuracy determines the eventual success or failure of computerized analysis procedures. Discontinuity and similarity are two basic properties of the pixels in relation to their local neighborhood used in many segmentation methods. The segmentation methods that are based on discontinuity property of pixels are considered as boundary or edges based techniques and that

are based on similarity are region based techniques (Verma et al., 2013). In the first category, the approach is to partition an image based on abrupt changes in intensity, such as edges. The principle approaches in the second category are based on partitioning an image into regions that are similar according to a set of predefined criteria, such as thresholding and clustering (Gonzalez and Woods, 2008). To be useful, these techniques must typically be combined with a domain's specific knowledge in order to effectively solve the domain's segmentation problems.

In recent years, some methods have been proposed for the segmentation of phytoplankton images. Jalba et al. (2004) proposed a marker-controlled watershed algorithm for automatic segmentation of diatom microscopic images, which improved initial segmentation results obtained within the ADIAC project (du Buf and Bayer, 2002; Fischer et al., 2002) and was applied in the further developed diatom image classification system (Dimitrovski et al., 2012). Blaschko et al. (2005) applied snake-based segmentation to produce the smooth closed contour and intensity-based segmentation to capture fine details of plankton from images obtained in situ by FlowCAM. Rodenacker et al. (2006) used threshold-based method to segment the aqueous specimens from microscopic images. Sosik and Olson (2007) applied simple threshold-based edge detection on phase congruency images generated by Imaging FlowCytobot to extract phytoplankton cell characteristics. Luo et al. (2011) used Canny edge detector followed by the robust regression method as the segmentation adjustment to find the

*Correspondence to: Haiyong Zheng; Department of Electronic Engineering, Ocean University of China, Qingdao, Shandong 266100, China. E-mail: zhenghaiyong@ouc.edu.cn

Received 10 April 2014; accepted in revised form 22 May 2014

REVIEW EDITOR: Prof. Alberto Diaspro

Contract grant sponsor: National Natural Science Foundation of China; Contract grant numbers: 61271406 and 61301240.

DOI 10.1002/jemt.22389

Published online 10 June 2014 in Wiley Online Library (wileyonlinelibrary.com).

circular diatom from microscopic images. Verikas et al. (2012) applied Fuzzy C-Means clustering algorithm to segment the circular objects representing the *Prorocentrum minimum* (*P. minimum*) species in phytoplankton microscopic images.

Analysis of the literature shows that the segmentation of phytoplankton from microscopic images performs well mainly on non-setae species. However, due to the noise and illumination variations while microscopic imaging, it is very hard to detect and segment the thin and long setae from the very low contrast background. Based on the characteristics of *Chaetoceros* microscopic images, this article presents a novel image processing model, named Grayscale Surface Direction Angle Model (GSDAM), to detect and segment the setae from *Chaetoceros* microscopic images for further image analysis tasks. Compared with the experimental results of both boundary-based and region-based segmentation methods using the subjective evaluation, our algorithm based on GSDAM performs better on the effectiveness and accuracy of setae segmentation.

MATERIALS AND METHODS

Image Acquisition

The *Chaetoceros* samples we used in this study were separated from China coastal waters such as Bohai Bay, Yellow Sea, East China Sea, and South China Sea. Most species were collected by “Dong Fang Hong 2” marine survey vessel of Ocean University of China and observed by Nikon Eclipse E800 biological research microscope in brightfield (BF) mode equipped with the CFI60 optical system and the Nikon Digital Sight camera for acquisition of *Chaetoceros* images which were snapped and stored digitally using Image Pro Plus software.

A small number of *Chaetoceros* species in this study were sampled from the Algal Collection of Research Center for Harmful Algae and Aquatic Environment in Jinan University, and they were mainly separated from the high frequency HAB (Harmful Algal Blooms) occurrence areas of South China Sea. The microscopic images of these samples were acquired using QImaging Retiga 4000R FAST 1394 CCD digital camera equipped on the Olympus BX61 microscope illuminated by a 12 V 100 W halogen light source in BF mode.

Image Characteristics

With the observation and analysis of considerable *Chaetoceros* microscopic images, we found that the setae in microscopic images were always thin and long but very close to the background on intensity due to the surrounding water or inappropriate focus (Figs. 1a and 1b), which made the boundary-based methods relying on discontinuity property of pixels such as the commonly used Canny edge detector inadequate for reliable automated setae segmentation. Besides, noise such as dust specks and debris with similar intensity of the setae (especially also close or connect to the setae) might be present in the images (Fig. 1a) to influence the correct setae segmentation using the region-based methods relying on similarity property of pixels such as thresholding and clustering.

Although the microscopic images are always acquired in color (24-bit pixel depth), it is hard to use the color information for setae segmentation because

the light source and filters can make the imaging color very different (as shown in Figs. 1a and 1b). In addition, we also found that some light and dark strips in particular angles appear on the areas around the setae in the microscopic images.

Grayscale Surface Direction Angle Model

Considering the setae characteristics in the microscopic images mentioned above, we developed a novel image processing model named GSDAM based on vector space theory combining with the grayscale surface of the image for setae detection and segmentation.

Due to the device-dependent imaging color information, the original RGB microscopic image is firstly converted to grayscale image using the MATLAB function “*rgb2gray*” with the image intensity (I) calculated by forming a weighed sum of the red (R), green (G), and blue (B) components according to the formula $I=0.2989\times R+0.5870\times G+0.1140\times B$. Then the grayscale image can be treated as a surface in the three dimensional Cartesian coordinate system (O-XYZ), where the X axis represents the image width, the Y axis represents the image height, and the Z axis represents the image intensity. Figure 1c is the converted grayscale image of the original RGB microscopic image Figure 1b, while Figure 1d shows the grayscale surface and its contours of the grayscale image Figure 1c plotted by the MATLAB function “*surf*.” The mostly horizontal grayscale surface in Figure 1d illustrates the low contrast background and the blue contours above the surface shows the cell with some missing setae. These contours also tell us that the grayscale surface contains the information of the cell as well as the setae (but only some missing setae from the contour lines).

To segment the setae from microscopic images, we created the GSDAM combing the intensity information of the adjacent pixels with the direction information of the surface composed of the adjacent pixels. The three dimensional coordinate system O-XYZ of grayscale image pixels is established shown in Figure 2, where (X, Y) is the spatial position of the pixel in the image and Z is the grayscale intensity of the pixel at coordinates (X, Y) . Given a pixel A with position (i, j) and intensity $I(i, j)$, the adjacent pixels used in our model are shown as $B(i, j+1)$, $C(i+1, j)$, and $D(i+1, j+1)$ with the intensity of $I(i, j+1)$, $I(i+1, j)$, and $I(i+1, j+1)$, respectively, corresponding to four points in three dimensional space shown in Figure 2: A' , B' , C' , and D' , which are located on the grayscale surface of the image.

Then our GSDAM can be summarized by the following steps:

1. Calculate the normal vector to the plane $A'C'B'$ by $\vec{f}_{A'C'B'} = \vec{A'C'} \times \vec{A'B'}$, where $\vec{A'C'} = (1, 0, I(i+1, j) - I(i, j))$ and $\vec{A'B'} = (0, 1, I(i, j+1) - I(i, j))$;
2. Use the same method to calculate the normal vectors to the planes $B'A'D'$, $D'B'C'$, and $C'D'A'$ represented by $\vec{f}_{B'A'D'}$, $\vec{f}_{D'B'C'}$, and $\vec{f}_{C'D'A'}$, respectively;
3. Estimate the normal vector to the grayscale surface at point A' by $\vec{f}_{A'} = (\vec{f}_{A'C'B'} + \vec{f}_{B'A'D'} + \vec{f}_{D'B'C'} + \vec{f}_{C'D'A'}) / 4$;
4. Calculate the angles between the normal vector $\vec{f}_{A'}$ with the coordinates (f_x, f_y, f_z) and the positive

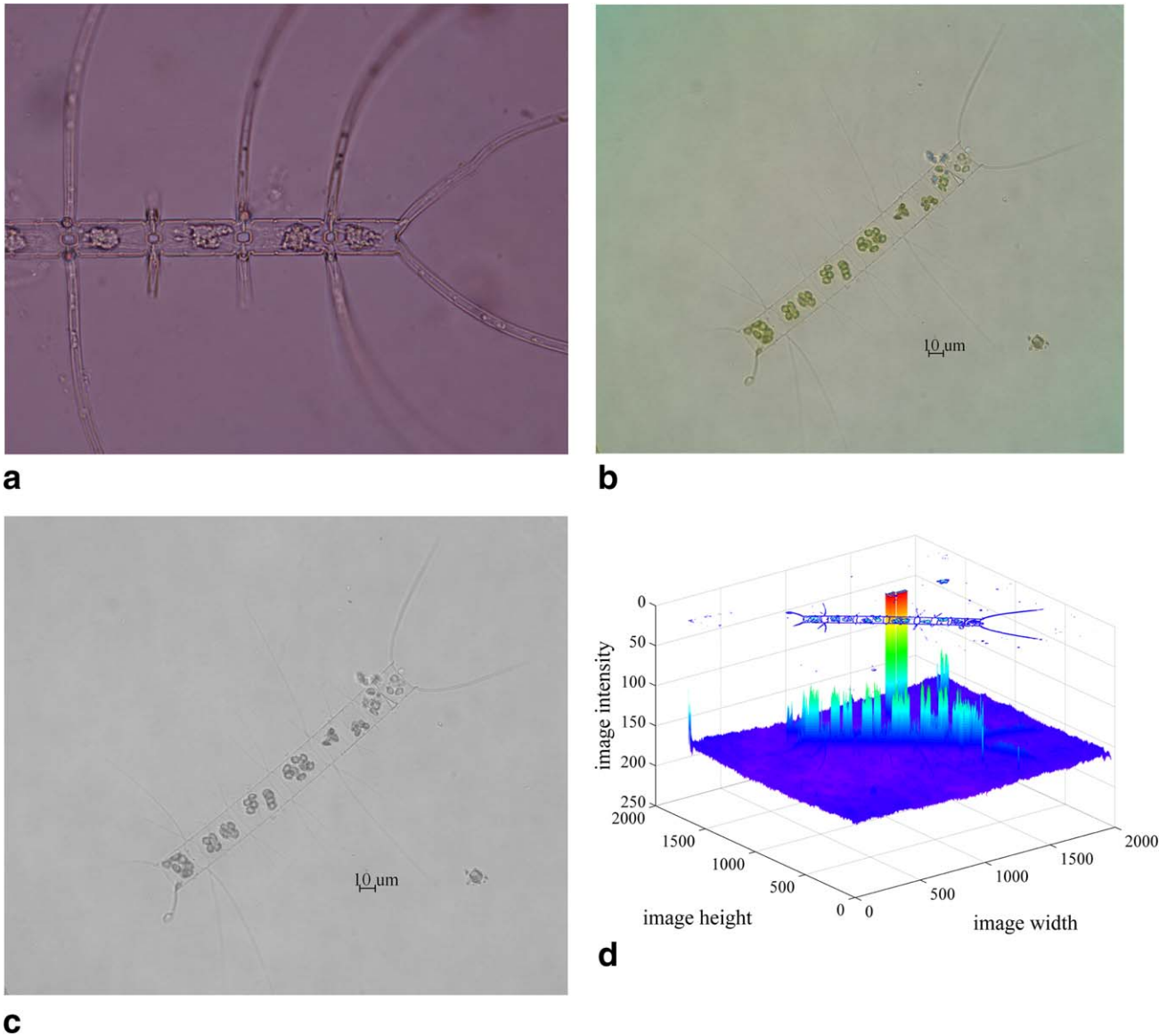


Fig. 1. (a) *Chaetoceros borealis* microscopic image. (b) *Chaetoceros lorenzianus* microscopic image. (c) Grayscale image of Figure 1b. (d) Grayscale surface with its contours of Figure 1c. [Color figure can be viewed in the online issue, which is available at wileyonlinelibrary.com.]

direction of the three coordinate axes X, Y, Z according to the direction cosines by the formulas ($|\vec{f}_{A'}|$ is the norm of the vector $\vec{f}_{A'}$):

$$\theta_x(i,j) = 360 \times \cos^{-1} \left(\frac{f_x}{|\vec{f}_{A'}|} \right) / 2\pi$$

$$\theta_y(i,j) = 360 \times \cos^{-1} \left(\frac{f_y}{|\vec{f}_{A'}|} \right) / 2\pi$$

$$\theta_z(i,j) = 360 \times \cos^{-1} \left(\frac{f_z}{|\vec{f}_{A'}|} \right) / 2\pi$$

5. Map the degrees of three direction angles in the range $[0,360]$ (actually in its subset $[\min(\theta), \max(\theta)]$ that $\min(\theta)$ and $\max(\theta)$ are the minimum and maximum direction degrees of the

normal vectors to the grayscale surface at all pixels in the image) to grayscale intensity values in the range $[0, 255]$ as follows:

$$Map_x(i,j) = 255 \times \frac{\theta_x(i,j) - \min(\theta_x)}{\max(\theta_x) - \min(\theta_x)}$$

$$Map_y(i,j) = 255 \times \frac{\theta_y(i,j) - \min(\theta_y)}{\max(\theta_y) - \min(\theta_y)}$$

$$Map_z(i,j) = 255 \times \frac{\theta_z(i,j) - \min(\theta_z)}{\max(\theta_z) - \min(\theta_z)}$$

6. Calculate $map_{xz}(i,j)$ and $map_{yz}(i,j)$ by $map_{xz}(i,j) = \sqrt{Map_x(i,j)^2 + Map_z(i,j)^2}$ and $map_{yz}(i,j) =$

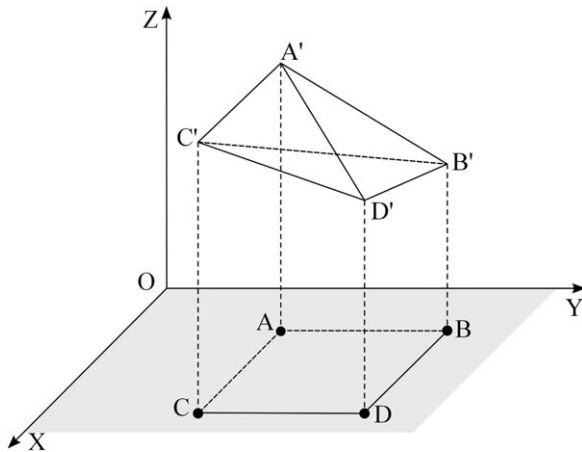


Fig. 2. Grayscale surface direction angle model (GSDAM).

$\sqrt{Map_y(i,j)^2 + Map_z(i,j)^2}$, respectively and also map them to grayscale intensity values $Map_{xz}(i,j)$ and $Map_{yz}(i,j)$ in the range $[0, 255]$ according to step 5;

7. Process all the pixels in the image using the same procedure of pixel A mentioned above to obtain the grayscale images Map_x , Map_y , Map_z , Map_{xz} , and Map_{yz} with the same size of the original RGB microscopic image. For the pixels on the right and lower edge of the image, we extend the edges by repeating the outer pixels.

For convenience, we take four pixels (corresponding to the four points A B C D in our model) in a binary image (the simple situation of a grayscale image that the grayscale intensity values are only 0 or 1) as an example to show the procedure and the results of GSDAM. We then classify all the cases depending on the pixel intensity value (0 for black and 1 for white) into five categories: all four black, all four white, two black and two white, one black and three white, one white and three black. According to the position of the black and white pixels, all the five categories can be further subdivided into 16 cases listed in Table 1 with the calculated mapping grayscale values of the corresponding Map_x , Map_y , Map_z , Map_{xz} , and Map_{yz} .

For the setae in microscopic images, their stretching directions from the cell with different pixel intensity values can be considered as the following six situations: horizontal, vertical, upper-right, lower-right, upper-left, and lower-left, which could be the combination constituted by the cases listed in line 2 to line 9 of Table 1. From Table 1 it can be seen that their corresponding mapping grayscale values of Map_{xz} and Map_{yz} are greater than those (0) of the other cases (line 1 in Table 1) which indicate the low contrast background (first two cases in line 1) as well as the noise without direction (last two cases in line 1). Therefore, Map_{xz} and Map_{yz} might be used to segment the setae while suppressing the background and noise.

To illustrate the results for images, Figure 3a shows an example binary image (the simple situation of a grayscale image) in size 256×256 created with four white rows and four white columns of pixels in the center of the black background as the original input image

TABLE 1. Cases of four pixels in a binary image with the corresponding mapping grayscale values

Cases	Map_x	Map_y	Map_z	Map_{xz}	Map_{yz}
	127	127	0	0	0
	255	127	255	255	172
	0	127	255	139	172
	127	255	255	172	255
	127	0	255	172	139
	196	196	200	167	167
	59	59	200	89	89
	196	59	200	167	89
	59	196	200	89	167

of our GSDAM. Map_x (Fig. 3b) and Map_y (Fig. 3c) illustrate the changes of pixel intensity in the vertical (height) and horizontal (width) direction of the image respectively, while Map_z (Fig. 3d) shows the changes of pixel intensity values regardless of the direction. Map_{xz} (Fig. 3e) and Map_{yz} (Fig. 3f) combine the pixel intensity values with the direction, which might be used to detect and segment the setae.

RESULTS

Setae Segmentation Based on GSDAM

The grayscale images of Map_{xz} and Map_{yz} in our GSDAM might contain the useful setae information as well as some useless noise, so we developed an algorithm (Fig. 4) to detect and segment the cell with setae while eliminating the background and noise from *Chaetoceros* microscopic images based on GSDAM.

The algorithm is summarized as follows:

1. Convert the color microscopic image to grayscale image;
2. Use our GSDAM on the grayscale image to output two grayscale images Map_{xz} and Map_{yz} ;
3. Apply bilateral filtering (Tomasi and Manduchi, 1998) for edge-preserving smoothing and Otsu's thresholding method (Otsu, 1979) for binarization on Map_{xz} and Map_{yz} , respectively, to eliminate some noise while keeping the useful cell and setae information yielding two binary images;
4. Implement logical AND operation (Russ, 2011) on the two binary images to combine the useful information from different directions and then median filtering (Huang et al., 1979) to reduce the noise located on only one of the two images while further highlighting the cell and setae;
5. Apply morphological closing operation (Russ, 2011) to smooth sections of contours, find, and fill the maximum area contour to extract the cell object with the setae and remove big chunks of noise, and morphological opening operation (Russ, 2011) to smooth the contour of the object yielding the final binary image (template) with the position of the cell and setae;
6. Implement logical AND operation (Russ, 2011) on the final binary image (template) and the original color microscopic images to obtain the final result of cell and setae segmentation.

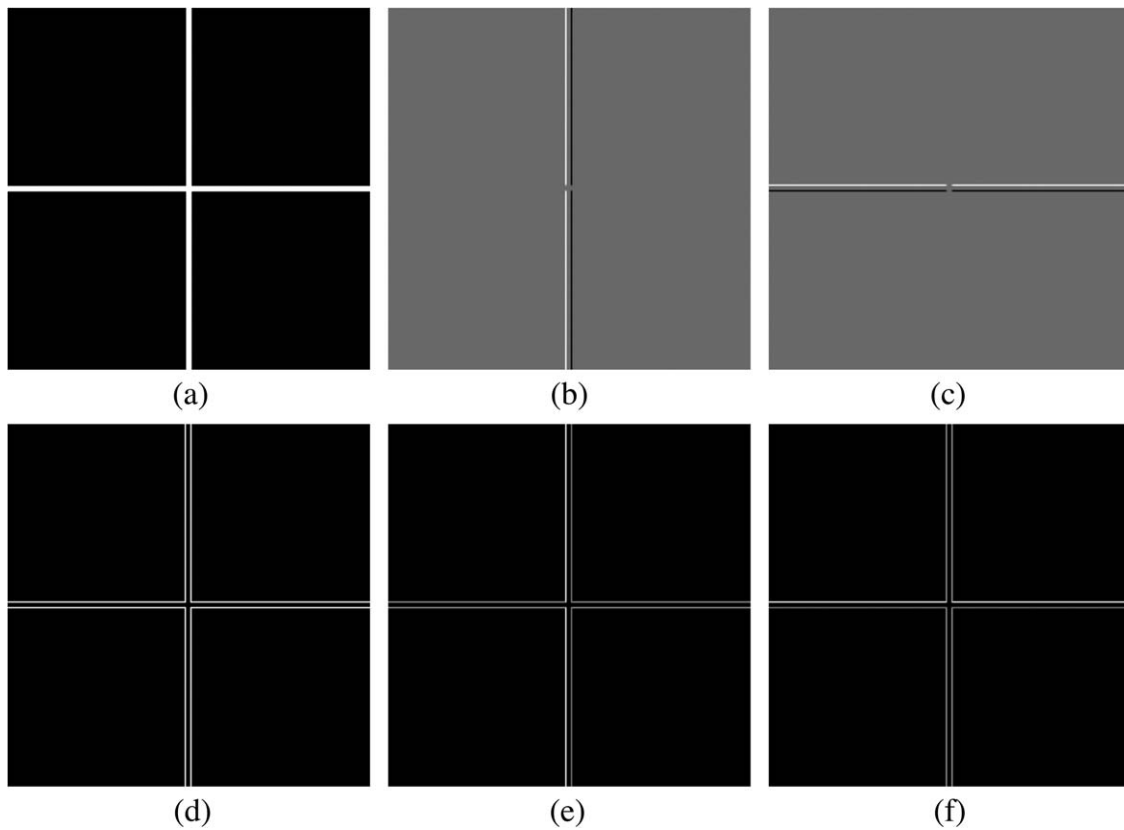


Fig. 3. An example to show the results of GSDAM. (a) Original image. (b) Map_x . (c) Map_y . (d) Map_z . (e) Map_{xz} . (f) Map_{yz} .

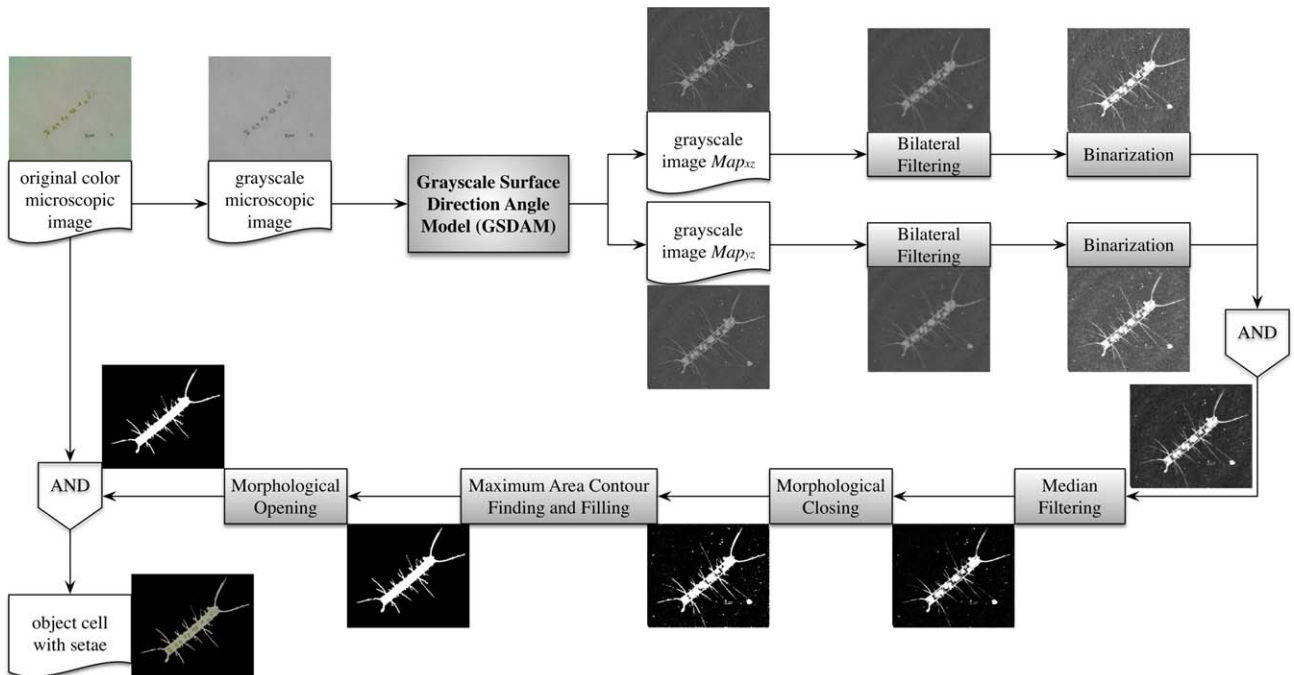


Fig. 4. The algorithm to segment setae from microscopic images based on GSDAM. [Color figure can be viewed in the online issue, which is available at wileyonlinelibrary.com.]

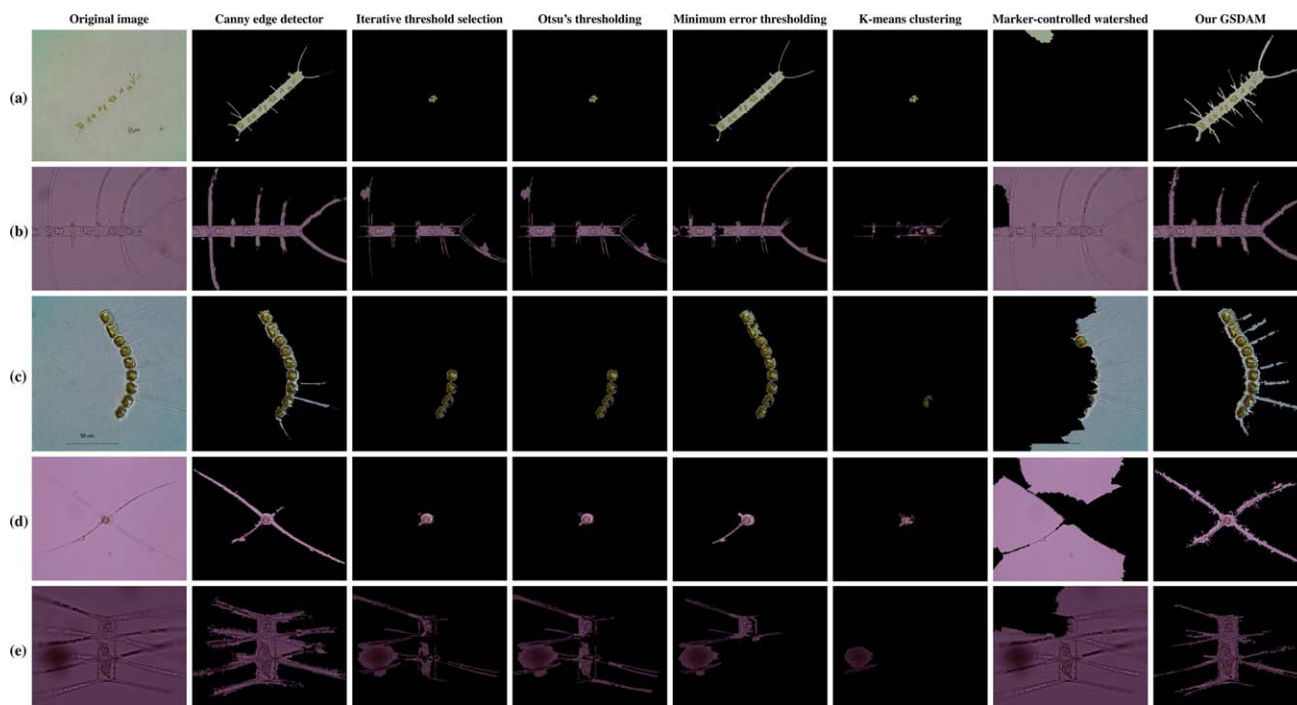


Fig. 5. Comparison with the commonly used boundary-based and region-based segmentation methods. The first column shows the original RGB microscopic images of the following *Chaetoceros* species in each row: (a) *Chaetoceros lorenzianus*. (b) *Chaetoceros borealis*. (c) *Chaetoceros curvisetus*. (d) *Chaetoceros danicus*. (e) *Chaetoceros castrocaniei*. For comparison, the remaining columns present the results

obtained by the following methods consecutively: Canny edge detector, iterative threshold selection, Otsu's thresholding, minimum error thresholding, K-means clustering, marker-controlled watershed, and our GSDAM. [Color figure can be viewed in the online issue, which is available at wileyonlinelibrary.com.]

Comparison with the Boundary-Based and Region-Based Methods

To test the performance of the proposed algorithm on setae segmentation from microscopic images, we applied the commonly used boundary-based and region-based segmentation methods Canny edge detector (Canny, 1986), iterative threshold selection (Ridler and Calvard, 1978), Otsu's thresholding (Otsu, 1979), minimum error thresholding (Kittler and Illingworth, 1986), K-means clustering (Hartigan and Wong, 1979), and marker-controlled watershed (Gonzalez and Woods, 2008) on the *Chaetoceros* microscopic images also for cell and setae segmentation. Besides, in order to find exactly the cell object which always occupies the largest area compared with the noise in the microscopic image, we used the similar post-processing of extracting the maximum area as the object to remove big chunks of noise, and the final experimental results are shown in Figure 5 (the first column shows the original RGB microscopic images and the remaining columns present the segmentation results obtained by the methods mentioned earlier and our GSDAM method consecutively). It can be seen that our GSDAM algorithm (the last column of Fig. 5) performs better on the effectiveness and accuracy of setae segmentation.

DISCUSSION

A novel image processing model GSDAM is presented for the separation of the setae-like information

from the background and the noise of images. Because the color of the microscopic image varies with the imaging device and the filters, our GSDAM uses the grayscale image converted from the color image. The idea behind GSDAM depends on the biomorphic characteristics of the setae in the low contrast microscopic images, which are always thin and long in a particular direction. Considering the grayscale surface of the image, the intensity values of the pixels on the setae are strongly related to those of the adjacent pixels on the same setae in a particular direction (line 2 to line 9 of Table 1), while the intensity values of pixels belong to background (first two cases in line 1 of Table 1) or noise (last two cases in line 1 of Table 1) are always isolated without direction. So our GSDAM tries to extract and combine the intensity and direction information of the surface formed by the four adjacent pixels based on vector space theory, which can be used to separate the setae from the background as well as the noise. Moreover, the connectivity and directionality of lineal structures (corresponding to the thin and long setae) can be kept while processing all the four adjacent pixels of the image (as shown in Fig. 3 for the simple situation). Furthermore, the focal influences of microscopic images can also be partly suppressed because of the extracted direction information (as shown in the first column of Figs. 5a and 5c for the inappropriate focus of setae and the last column for the extracted setae respectively).

In this article, the algorithm based on GSDAM is developed for the setae segmentation from *Chaetoceros*

microscopic images. The grayscale images of Map_{xz} and Map_{yz} from our GSDAM followed by a post-processing procedure (Fig. 4) are adopted to segment setae from microscopic images. As shown in Figure 5, it's obvious to see that the thresholding (column 3 to column 5) and clustering (column 6) methods are almost ineffective to segment the setae even the cell because of the low contrast *Chaetoceros* microscopic images. Among the region-based segmentation methods, the minimum error thresholding method performs well on segmenting cell as well as a few setae (column 5 of Fig. 5b), but it's hard to process the strong noise produced by dust specks and debris (column 5 of Fig. 5e). It also can be seen that the Canny edge detector (column 2 of Fig. 5) can segment the setae better than region-based methods but less complete and accurate than our GSDAM. The marker-controlled watershed method (column 7 of Fig. 5) performs worst because the results depend on the marker selection as well as the image characteristics. Although it could be useful for non-setae phytoplankton image segmentation (Jalba et al., 2004), it's hard to design an appropriate marker selection scheme for the low contrast *Chaetoceros* microscopic images to segment the setae and the cell.

Although our algorithm based on GSDAM has performed well in the experiments shown in Figure 5, it does need more effort on the setae segmentation more accurately and completely in the future. First, in the proposed algorithm, only Map_{xz} and Map_{yz} from GSDAM are selected to segment the setae. However, we have noted that the other mapping grayscale images may also contain meaningful setae information. Second, different post-processing procedure can lead to different setae segmentation result. Therefore, much better performance can be obtained by the more suitable post-processing. Third, the maximum area extraction in the post-processing procedure limits the segmentation used for single cell, which does not work in the case of the microscopic image with multiple *Chaetoceros* cells that needs to identify all the cells and the noise. The ultimate goal of our research is to develop a system for on-site and in situ real-time automatic identification and classification of *Chaetoceros* species.

ACKNOWLEDGMENT

The authors wish to thank the Algal Collection of Research Center for Harmful Algae and Aquatic Environment in Jinan University and Key Laboratory of Marine Environment and Ecology, Ministry of Education in Ocean University of China for providing the samples of *Chaetoceros* species and the instruments to observe and acquire the corresponding microscopic

images. The authors also would like to thank the anonymous referees for valuable criticisms and useful suggestions that helped us to improve the quality of our present and future work.

REFERENCES

- Blaschko MB, Holness G, Mattar MA, Lisin D, Utgoff PE, Hanson AR, Schultz H, Riseman EM. 2005. Automatic in situ identification of plankton. *IEEE WACV/MOTIONS* 1:79–86.
- Canny J. 1986. A computational approach to edge detection. *IEEE Trans Pattern Anal* 6:679–698.
- Dimitrovski I, Kocev D, Loskovska S, Dzeroski S. 2012. Hierarchical classification of diatom images using ensembles of predictive clustering trees. *Ecol Inform* 7:19–29.
- du Buf H, Bayer MM. 2002. Automatic diatom identification. Singapore: World Scientific.
- Fischer S, Shahbazkia HR, Bunke H. 2002. Contour extraction. In: Automatic diatom identification. du Buf H, Bayer MM, editors. Singapore: World Scientific. pp. 93–107.
- Gonzalez RC, Woods, RE. 2008. Image segmentation. In: Digital image processing. Upper Saddle River, New Jersey: Prentice Hall. pp. 689–794.
- Hartigan JA, Wong MA. 1979. Algorithm AS 136: A k-means clustering algorithm. *J R Stat Soc C* 28:100–108.
- Huang T, Yang G, Tang G. 1979. A fast two-dimensional medial filtering algorithm. *IEEE Trans Acoust Speech Signal Process* 27: 13–18.
- Jalba AC, Wilkinson MHF, Roerdink JBTM. 2004. Automatic segmentation of diatom images for classification. *Microsc Res Techniq* 65:72–85.
- Kittler J, Illingworth J. 1986. Minimum error thresholding. *Pattern Recogn* 19:41–47.
- Lee SD, Lee JH. 2011. Morphology and taxonomy of the planktonic diatom *Chaetoceros* species (Bacillariophyceae) with special intercalary setae in Korean coastal waters. *Algae* 26:153–165.
- Luo Q, Gao Y, Luo J, Chen C, Liang J, Yang C. 2011. Automatic identification of diatoms with circular shape using texture analysis. *J Softw* 6:428–435.
- Otsu N. 1979. A threshold selection method from gray-level histograms. *IEEE Trans Syst Man Cybern* 9:62–66.
- Ridler TW, Calvard S. 1978. Picture thresholding using an iterative selection method. *IEEE Trans Syst Man Cybern* 8:630–632.
- Rodenacker K, Hense B, Jütting U, Gais P. 2006. Automatic analysis of aqueous specimens for phytoplankton structure recognition and population estimation. *Microsc Res Techniq* 69:708–720.
- Russ JC. 2011. Processing binary images. In: The image processing handbook. Boca Raton: CRC Press. pp. 443–510.
- Shevchenko OG, Orlova TY. 2010. Morphology and ecology of the bloom-forming diatom *Chaetoceros contortus* from Peter the Great Bay, Sea of Japan. *Russ J Mar Biol* 36:243–251.
- Sosik HM, Olson RJ. 2007. Automated taxonomic classification of phytoplankton sampled with imaging-in-flow cytometry. *Limnol Oceanogr-Meth* 5:204–216.
- Tabassum A, Saifullah SM. 2010. The planktonic diatom of the genus *Chaetoceros* Ehrenberg from northwestern Arabian Sea bordering Pakistan. *Pak J Bot* 42:1137–1151.
- Tomasi C, Manduchi R. 1998. Bilateral filtering for gray and color images. *International Conference on Computer Vision*. pp. 839–846.
- Verikas A, Gelzinis A, Bacauskiene M, Olenina I, Olenin S, Vaiciukynas E. 2012. Phase congruency-based detection of circular objects applied to analysis of phytoplankton images. *Pattern Recogn* 45:1659–1670.
- Verma S, Khare D, Gupta R, Chandel GS. 2013. Analysis of image segmentation algorithms using MATLAB. *ITC*. pp. 163–172.